FOREVER YOUNG FLOWER Negatively Regulates Ethylene Response DNA-Binding Factors by Activating an Ethylene-Responsive Factor to Control Arabidopsis Floral Organ Senescence and Abscission[1]

Wei-Han Chen[2], Pei-Fang Li[2], Ming-Kun Chen, Yung-I Lee, and Chang-Hsien Yang*

Institute of Biotechnology (W.-H.C., P.-F.L., M.-K.C., C.-H.Y.) and Agricultural Biotechnology Center (C.-H.Y.), National Chung Hsing University, Taichung, Taiwan 40227, Republic of China; and Biology Department, National Museum of Natural Science, Taichung, Taiwan 40227, Republic of China (Y.-I.L.)

ORCID IDs: 0000-0002-6295-8543 (W.-H.C.); 0000-0002-9150-4436 (M.-K.C.).

In this study of Arabidopsis (*Arabidopsis thaliana*), we investigated the relationship between *FOREVER YOUNG FLOWER* (*FYF*) and *Ethylene Response DNA-binding Factors* (*EDFs*) and functionally analyzed a key *FYF* target, an *Ethylene-Responsive Factor* (*ERF*), that controls flower senescence/abscission. Ectopic expression of *EDF1/2/3/4* caused promotion of flower senescence/abscission and the activation of the senescence-associated genes. The presence of a repressor domain in EDFs and the enhancement of the promotion of senescence/abscission in *EDF1/2/3/4+SRDX* (converting EDFs to strong repressors by fusion with the ERF-associated amphiphilic repression motif repression domain SRDX) transgenic plants suggested that EDFs act as repressors. The significant reduction of β-glucuronidase (GUS) expression by *35S:FYF* in *EDF1/2/3/4:GUS* plants indicates that *EDF1/2/3/4* functions downstream of *FYF* in regulating flower senescence/abscission. In this study, we also characterized an *ERF* gene, *FOREVER YOUNG FLOWER UP-REGULATING FACTOR1* (*FUF1*), which is up-regulated by *FYF* during flower development. Ectopic expression of *FUF1* caused similar delayed flower senescence/abscission as seen in *35S:FYF* plants. This phenotype was correlated with deficient abscission zone formation, ethylene insensitivity, and down-regulation of *EDF1/2/3/4* and abscission-associated genes in *35S:FUF1* flowers. In contrast, significant promotion of flower senescence/abscission and up-regulation of *EDF1/2/3/4* were observed in *35S:FUF1+SRDX* transgenic dominant-negative plants, in which FUF1 is converted to a potent repressor by fusion to an SRDX-suppressing motif. Thus, FUF1 acts as an activator in suppressing *EDF1/2/3/4* function and senescence/abscission of the flowers. Our results reveal that *FYF* regulates flower senescence/abscission by negatively regulating *EDF1/2/3/4*, which is the downstream gene in the ethylene response, by activating *FUF1* in Arabidopsis.

Senescence and abscission of floral organs usually occur after pollination. However, these two processes are not perfectly coupled during flower development, suggesting that both overlapping and independent regulations exist (Rogers, 2013). The processes of flower senescence and abscission, which are triggered by pollination, are primarily controlled by two hormones: ethylene and auxin (Roberts et al., 2002; Rogers, 2013). In Arabidopsis (*Arabidopsis thaliana*), ethylene accelerates flower senescence/abscission, and mutations in the genes involved in the ethylene signaling pathway, such as *ethylene receptor1* (*etr1*) and *ethylene insensitive2* (*ein2*), cause delayed senescence and abscission (Patterson and Bleecker, 2004; Graham et al., 2012). By contrast, a mutation in the *CONSTITUTIVE TRIPLE RESPONSE1* (*CTR1*) gene causes a constitutive ethylene response and early senescence and abscission of the flowers (Kieber et al., 1993; Huang et al., 2003). Auxin is thought to inhibit senescence and abscission (Roberts et al., 2002; Basu et al., 2013).

Although the key genes involved in the Arabidopsis ethylene signaling pathway have been identified (Chen et al., 2005; Wang et al., 2013), the putative functions of the candidate downstream genes induced by this pathway, such as the Ethylene Response Factor (ERF)/APETALA2 (AP2) transcription factors, which include ERFs and the Ethylene Response DNA-binding Factors (EDFs; Alonso et al., 2003; Stepanova and Alonso, 2005; Castillejo and Pelaz, 2008; Xu et al., 2011; Schaller, 2012), still remain to be investigated. A possible

role for *EDF* as a downstream gene in the ethylene response was supported by several recent reports (Woo et al., 2010; Chen et al., 2011; Lumba et al., 2012; Chang et al., 2013). It has been shown that *EDF1/2* was down-regulated in plants that ectopically expressed *FOREVER YOUNG FLOWER* (*FYF*), which caused the delay of flower senescence and abscission and ethylene insensitivity (Chen et al., 2011). *EDF* genes have also been reported to be regulated by *FUSCA3* (*FUS3*), which regulates the vegetative-phase transitions (Lumba et al., 2012). *EDF2/4* expression was up-regulated, and the protein stability of a key transcriptional regulator of ethylene signaling, EIN3, was increased in germinating *fus3* mutants (Lumba et al., 2012). The increased levels of the *EDF* transcripts in the *fus3* mutants were partially suppressed by treatment with an ethylene signaling inhibitor: silver ions (AgNO$_3$; Lumba et al., 2012). Interestingly, EDF4/RELATED TO ABI3/VP1 1 (RAV1) has been shown to be involved in regulating leaf senescence (Woo et al., 2010). Furthermore, it has been reported that EIN3 could bind to the promoters of *EDF1/2/3/4* (Chang et al., 2013). Although these results suggest that the *EDF* genes may be regulated by *FYF*, *FUS3*, and *EIN3* in distinct developmental processes (Chen et al., 2011; Lumba et al., 2012; Schaller, 2012; Chang et al., 2013), another functional analysis of the *EDF* genes is required to determine if they play a role in regulating senescence and abscission or vegetative-phase transitions in the downstream steps of the ethylene response.

In delaying flower senescence and abscission, *FYF* not only suppresses *EDF* expression but also, negatively regulates some abscission-associated genes, including *BLADE-ON-PETIOLE2* (*BOP2*) and *INFLORESCENCE DEFICIENT IN ABSCISSION* (*IDA*; Chen et al., 2011). *BOP1/2* is necessary for the formation of the floral abscission zone (AZ; Hepworth et al., 2005; Norberg et al., 2005; McKim et al., 2008; Wu et al., 2012), whereas IDA proteins interact with the receptor-like kinases HAESA (HAE) and HAESA-LIKE2 (HSL2) to control the abscission initiation of floral organs (Cho et al., 2008; Stenvik et al., 2008; Shi et al., 2011; Liljegren, 2012). The functions of *BOP1/2* and *IDA* are thought to be independent of enzymes, such as polygalacturonase, that may be involved in AZ cell wall degradation (Roberts et al., 2002; Gonzalez-Carranza et al., 2007a, 2012). Thus, *FYF* inhibits flower senescence and abscission through both ethylene-dependent and -independent pathways (Chen et al., 2011; Rogers, 2013).

To further validate the relation between the *EDFs* and *FYF* in the ethylene signaling pathway, a functional analysis of the *EDF* genes was performed in this study. We showed that *EDF1/2/3/4* functioned as a repressor to cause the senescence and abscission in flower organs by suppressing a mechanism that suppresses senescence and abscission in the ethylene signaling pathway. To further delineate the mechanisms regulated by *FYF*, we identified and investigated an *ERF* gene (termed *FOREVER YOUNG FLOWER UP-REGULATING FACTOR1* [*FUF1*]; At1g71450) in

this study. We showed that ectopically expressing *FUF1* caused ethylene insensitivity and delayed the senescence/abscission of the floral organs by suppressing the *EDFs*, *BOP1/2*, and *IDA/HAE/HSL2/HAWAIIAN SKIRT* (*HWS*). The promotion of flower senescence/abscission in *FUF1+SRDX* plants, which are transgenic dominant-negative mutants, in which *FUF1* is converted to a potent repressor by fusion to an SRDX-suppressing motif (Chen et al., 2011), further supported the idea that *FUF1* acts as an activator in promoting a mechanism that suppresses senescence/abscission. Our findings further extend the knowledge regarding the pathway by which *FYF* suppresses *EDF1/2/3/4*, the downstream gene in the ethylene signaling pathway, by activating the *ERF* gene *FUF1* in Arabidopsis.

RESULTS

The Detection of *EDF* Expression during Flower Development

The EDF1/2/3/4 proteins contain ERF/AP2 and B3 DNA-binding domains and belong to the RAV subfamily of ERF/AP2-related proteins (Supplemental Fig. S1; Sakuma et al., 2002; Nakano et al., 2006). To investigate the expression patterns of the *EDF1/2/3/4* genes, *EDF1/2/3/4:GUS* plants were obtained. In contrast with *FYF:GUS* flowers, in which strong GUS staining was detected in the sepals and petals of young flower buds and weaker staining decreased in young and mature flowers (Chen et al., 2011; Supplemental Fig. S2), the GUS activity of the *EDF1:GUS* flowers was not detected during the early flower development stages (before stage 8), and their expression increased from stage 9 to the late developmental stages (Supplemental Fig. S3A). Similar GUS staining pattern was observed in plants carrying *EDF2:GUS* (Supplemental Fig. S3B), *EDF3:GUS* (Supplemental Fig. S3C), and *EDF4:GUS* (Supplemental Fig. S3D), respectively. When the expression of *EDF1/2/3/4* in flowers in different developmental stages was further analyzed, significantly higher expression of *EDF1/2/3/4* was observed in late flower development (after stage 12) than in early development stages (before stage 9; Supplemental Fig. S3, E–H). These results indicated that the temporal expression patterns of *EDF1/2/3/4* were the opposite of those patterns of *FYF* during flower development.

The Ectopic Expression of *EDFs* Promotes Flower Senescence and Abscission in Transgenic Arabidopsis Plants

To investigate the functions of the *EDF* genes, the *35S:EDF1/2/3/4* was transformed into Arabidopsis. Of 140 kanamycin-resistant plants analyzed for each construct, 47, 59, 59, and 43 plants displayed flower senescence and abscission promotion for *35S:EDF1*, *35S:EDF2*, *35S:EDF3*, and *35S:EDF4*, respectively (Supplemental Table S1).

Figure 1. The ectopic expression of the *EDF*s and the *EDF*+*SRDX* constructs promotes flower senescence and abscission. A, The flowers along the inflorescence of the wild-type (WT; row 1), *35S:EDF1* (row 2), *35S:EDF2* (row 3), *35S:EDF3* (row 4), and *35S:EDF4* (row 5) plants. The numbers indicate the positions of the flowers. B to D, The perianth organs of the wild-type flowers (B) senesced and abscised after position 5 (arrow), whereas the perianth organs were completely senescent and abscised after position 3 (arrows) in *35S:EDF2* (C) and *35S:EDF4* (D) flowers. E, A schematic representation of the *EDF*+*SRDX* constructs. The red box indicates the conserved repressor sequence (RLFGV), and the green box indicates the SRDX domain (LDLDLELRLGFA). NLS, Nucleus localization signal. F, The flowers along the inflorescences of *ctr1* (row 1), *35S:EDF1*+*SRDX* (row 2), *35S:EDF2*+*SRDX* (row 3), *35S:EDF3*+*SRDX* (row 4), and *35S:EDF4*+*SRDX* (row 5) plants. G and H, The inflorescence stems of *35S:EDF1*+*SRDX* (G) and *35S:EDF4*+*SRDX* (H) plants. The perianth organs were completely senescent and abscised after position 2 (arrows) flowers.


The perianths of wild-type flowers abscised at approximately position 5 (Fig. 1, A and B), whereas the perianth organs of the *35S:EDF1/2/3/4* flowers senesced and abscised at positions 3 and 4 (Fig. 1, A, C, and D). The position was counted starting from the first flower with visible white petals at the top of the inflorescence (Bleecker and Patterson, 1997), and flower organ senescence and abscission were measured as described previously (Chen et al., 2011). Although the *35S:EDF1/2/3/4* perianth organs were completely senescent and abscised from the base of the flower after positions 3 and 4, these organs remained hanging on the siliques (Fig. 1A), even after these organs had been abscised from the flowers for 2 weeks (Fig. 1, A, C, and D). This phenotype resembled that observed in the *ctr1* mutants (Fig. 1F),

which have been shown to cause a constitutive ethylene response.

35S:EDFs+*SRDX* Transgenic Arabidopsis Exhibits Enhanced Promotion of Flower Senescence and Abscission

When the sequences of EDF1/2/3/4 proteins were analyzed, a conserved RLFGV sequence, similar to that of the ERF/AP2 repressors (Ikeda and Ohme-Takagi, 2009), was identified in the C-terminal region (Fig. 1E; Supplemental Fig. S1). The presence of this sequence indicated that the *EDF1/2/3/4* genes might encode transcriptional repressors. To examine this assumption, a conserved SRDX-suppressing motif that contains a 12-amino acid repressor sequence (LDLDLELRLGFA;
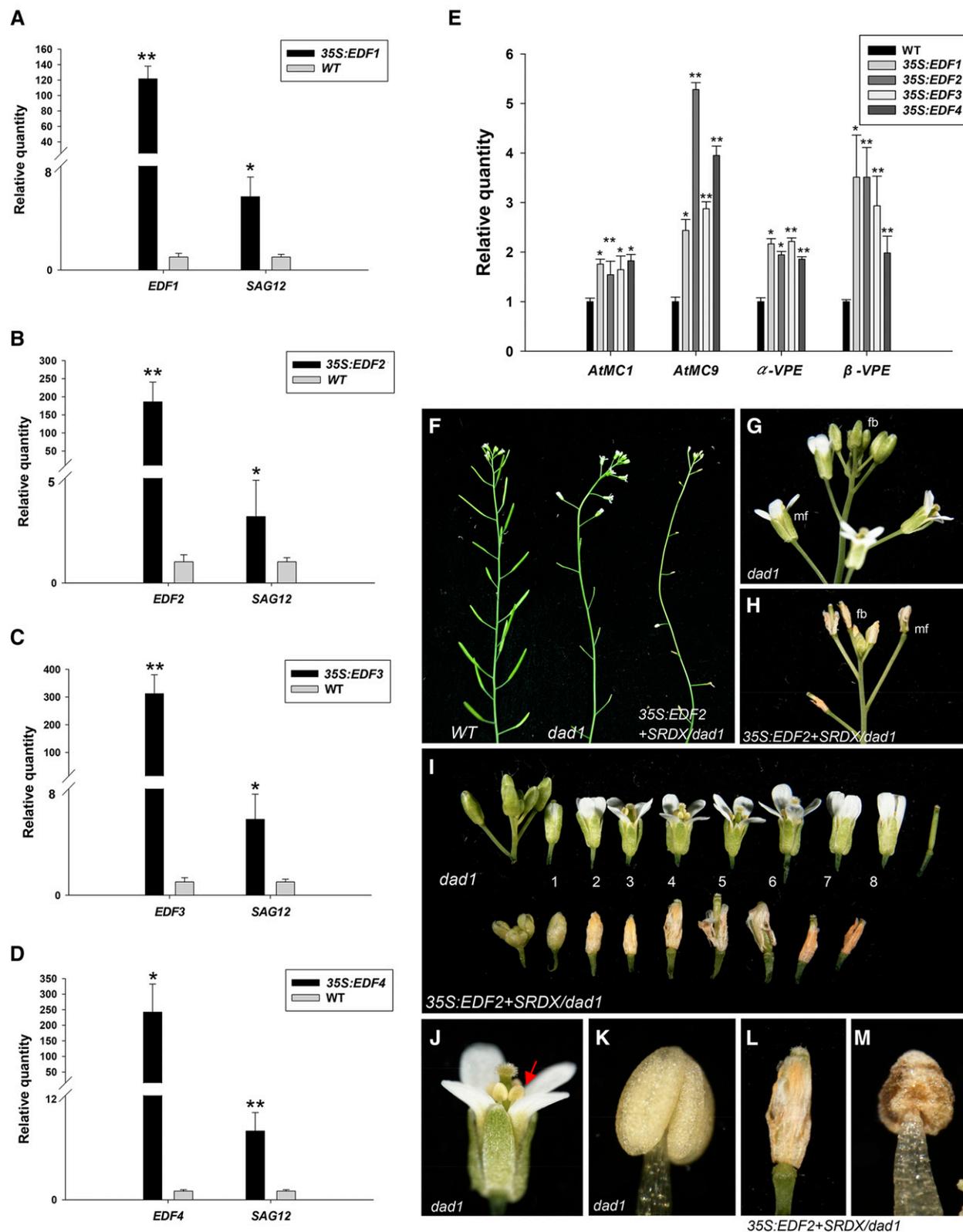
Figure 2. The detection of senescence-associated gene expression in *35S:EDF* plants and a phenotypic analysis of flower senescence and abscission in *dad1* plants ectopically expressing the *EDF2+SRDX* gene. A to D, The expression of the *SAG12* gene in *35S:EDF1* (A), *35S:EDF2* (B), *35S:EDF3* (C), and *35S:EDF4* (D) plants. E, The expression of *AtMC1*, *AtMC9*, *α-VPE*, and *β-VPE* genes in *35S:EDF* plants. The mRNA levels were determined by real-time quantitative PCR. Total RNA was isolated from

Chen et al., 2011) was fused to EDF1/2/3/4 (*EDF1/2/3/4+SRDX*; Fig. 1E). We expected that the overexpression of *EDF1/2/3/4+SRDX* would enhance the repression, resulting in a more severe phenotype than that observed in the *35S:EDF1/2/3/4* plants.

Of the 180 kanamycin-resistant plants analyzed for each construct, 52, 60, 68, and 59 plants showed the same abnormal phenotype for *35S:EDF1+SRDX*, *35S:EDF2+SRDX*, *35S:EDF3+SRDX*, and *35S:EDF4+SRDX*, respectively (Supplemental Table S2). Interestingly, senescence and abscission of the perianths of the *35S:EDF1/2/3/4+SRDX* plants (Fig. 1F) were enhanced compared with plants carrying *35S:EDF1/2/3/4* (Fig. 1A). The perianths of the *35S:EDF1/2/3/4+SRDX* flowers senesced and abscised at positions 2 and 3 (Fig. 1, F–H), which were earlier than in *35S:EDF1/2/3/4* flowers (position 3 and 4) or wild-type flowers (position 5; Fig. 1A). The completely senescent perianth organs that abscised from the base of the flowers after position 2 remained hanging on the *35S:EDF1/2/3/4+SRDX* siliques (Fig. 1, F–H) for several weeks, such as in the *ctr1* mutants (Fig. 1F). These results support the hypothesis that EDF1/2/3/4 plays a repressor role in regulating flower senescence and abscission.

Senescence-Associated Gene12 and Programmed Cell Death-Associated Gene Expression Levels Are Up-Regulated in Plants Carrying 35S:EDFs and 35S:EDFs+SRDX

Because flower senescence and abscission were promoted in *35S:EDFs+SRDX* transgenic Arabidopsis, thus, we analyzed the expression of senescence marker gene *senescence-associated gene12* (*SAG12*; Noh and Amasino, 1999) and the marker genes for programmed cell death (PCD), such as vacuolar processing enzymes (*VPEs*; with caspase-1 activity) and Metacaspase (*MCs*) genes (Rojo et al., 2004; Wagstaff et al., 2009; Coll et al., 2010) in *35S:EDFs* and *35S:EDFs+SRDX* plants. The result indicated that the expressions of *SAG12*, *AtMC1*, *AtMC9*, α-*VPE*, and β-*VPE* were significantly upregulated in *35S:EDFs* (Fig. 2, A–E) and *35S:EDF1/2/3/4+SRDX* plants (Supplemental Fig. S4, A–E). Thus, *35S:EDFs* promoted the senescence and abscission of the flower organs by activating senescence- and PCD-associated genes.

35S:EDF2+SRDX Promotes Flower Senescence and Abscission Independent of the Male Sterility Phenotype in *defective in anther dehiscence1* Mutants

The ectopic expression of *EDF1/2/3/4* clearly affects flower organ senescence and abscission and seems to render plants sterile, because delayed or no silique elongation was also observed in *35S:EDFs* and *35S:EDFs+SRDX* transgenic plants (Fig. 1, A and F). If the ectopic expression of *EDF1/2/3/4* does affect fertility, then this expression might have a consequence on the timing of floral organ senescence and abscission. To exclude this possibility, we generated transgenic plants containing *35S:EDF2+SRDX* in male sterility mutant *defective in anther dehiscence1* (*dad1*), which has defects in anther dehiscence (Fig. 2, F, J, and K; Ishiguro et al., 2001). The senescence/abscission of the *dad1* flowers was slightly delayed compared with the senescence/abscission of wild-type flowers (Fig. 2, F, G, and I). The result indicated that, in addition to producing a male sterility phenotype (Fig. 2, F, L, and M), a significant promotion of senescence and abscission was observed in *35S:EDF2+SRDX/dad1* flowers (Fig. 2, H, I, and L), similar to that observed for *35S:EDF2+SRDX* transgenic plants (Fig. 1F). This result strongly indicated that the *35S:EDF*-induced early senescence/abscission of the flower organs was not caused by the effect of the male sterility.

35S:EDFs+SRDX Constructs Promote Flower Senescence and Abscission in the *etr1* and *ein2* Mutants

To further confirm the relation between *EDF1/2/3/4* and the ethylene signaling pathway, the *35S:EDF1/2/3/4+SRDX* constructs were separately transformed into the Arabidopsis ethylene-insensitive mutants *etr1* and *ein2*, in which floral senescence and abscission are delayed to approximately position 8 (Supplemental Figs. S5A and S6A; Bleecker et al., 1988; Ecker, 1995; Patterson and Bleecker, 2004). The phenotypes of *35S:EDF1/2/3/4+SRDX/etr1-1* plants resembled the phenotypes of the *35S:EDF1/2/3/4+SRDX* plants. These plants displayed earlier senescence/abscission of the perianth organs (positions before 3 and 4) than the senescence/abscission of the *etr1-1* mutants (position 8; Supplemental Fig. S5, A–C; Supplemental Table S3). The promotion of

Figure 2. (*Continued.*)
the floral buds and the open flowers at positions 1 to 3 from one wild-type (WT) Col-0 plant and one *35S:EDFs* plant. The transcript levels of these genes were determined using two to three replicates and normalized using *UBQ10*. The expression of each gene is given relative to that of the wild-type plant, which was set at one. The asterisks in A to E indicate a significant difference from the wild-type value. *, $P \leq 0.05$; **, $P \leq 0.01$. F, The inflorescences of wild-type (left), *dad1* (center), and *35S:EDF2+SRDX/dad1* (right) plants. No silique elongation was observed in *dad1* and *35S:EDF2+SRDX/dad1* plants. G and H, Close-up of the flower buds (fbs) and mature flowers (mfs) for *dad1* (G) and *35S:EDF2+SRDX/dad1* (H) plants from F. I, The flowers along an inflorescence of the *dad1* (upper) and *35S:EDF2+SRDX/dad1* (lower) plants. The perianth organs did not senesce and abscised after position 8 for *dad1* mutants. The numbers indicate the positions of the flowers. The perianth organs of the flowers in *35S:EDF2+SRDX/dad1* plants were completely senescent and abscised at positions 2 and 3. J and K, Close-up view of a mature flower at position 4 (J) and an indehiscent anther (K) for the *dad1* plant from I. An arrow indicates the indehiscent anthers in J. L and M, Close-up view of a mature flower at position 4 (L) and an indehiscent anther (M) of the *35S:EDF2+SRDX/dad1* plant from I. Expression statistical analysis was measured by Student's *t* test (each *n* = 3).
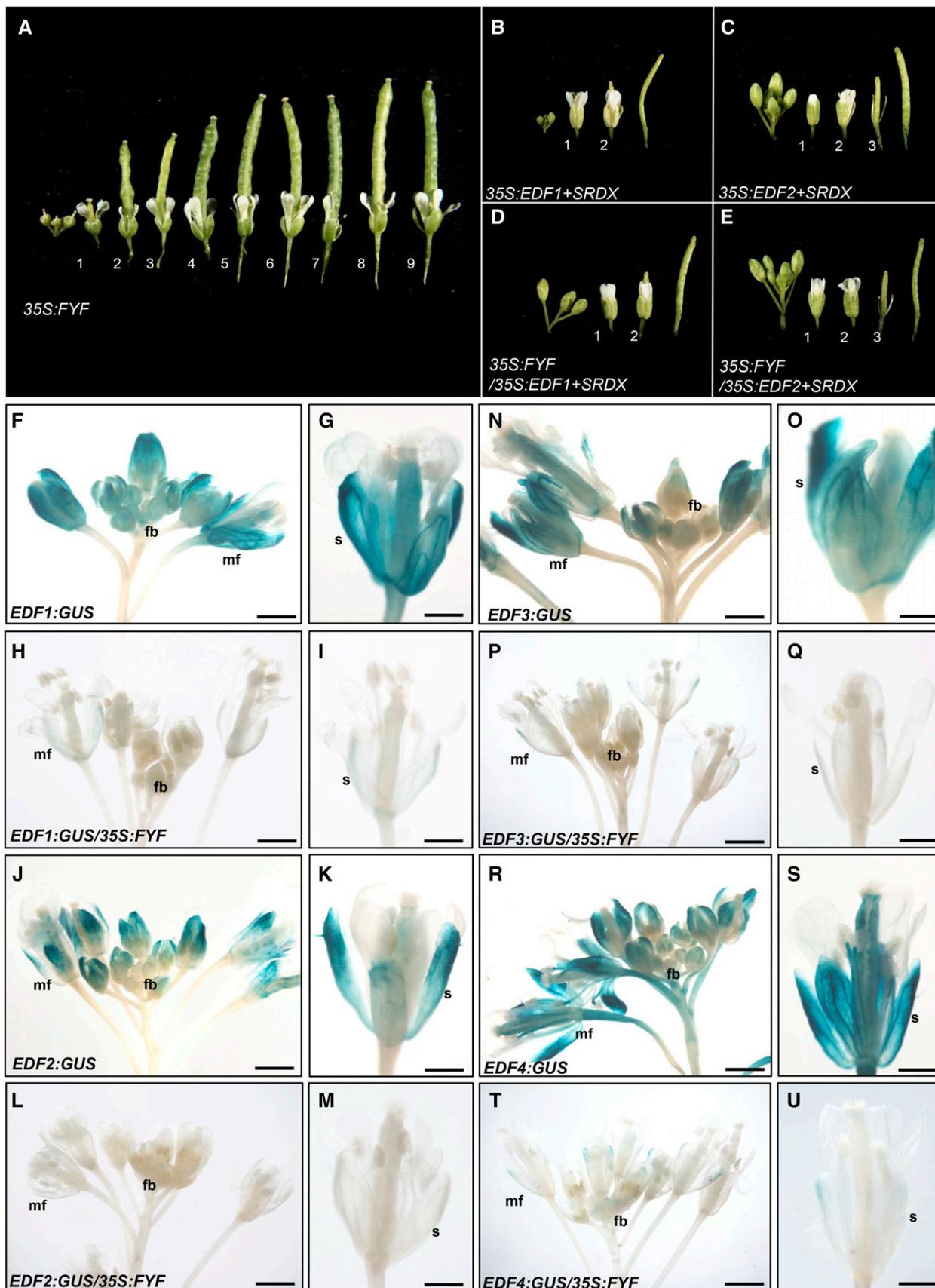
Figure 3. A phenotypic analysis of flower senescence and abscission in *35S:FYF* plants ectopically expressing the *EDF1,2+SRDX* genes and GUS staining patterns in *EDF*s:*GUS* plants ectopically expressing *35S:FYF*. A, The perianth organs did not senesce and abscised after position 9 of the *35S:FYF* inflorescence. B to E, Inflorescence stems

floral senescence and abscission in *35S:EDF1/2/3/4+ SRDX/etr1-1* correlated with the expression of *EDF1/2/ 3/4+SRDX* (Supplemental Fig. S5, D–G). Similarly, earlier senescence/abscission of the perianth organs was observed (positions before 3–5) for *35S:EDF1/2/3/ 4+SRDX/ein2-1* than for the *ein2-1* mutants (position 8; Supplemental Fig. S6, A–C; Supplemental Table S4). The promotion of floral senescence/abscission for *35S:EDF1/ 2/3/4+SRDX/ein2-1* also correlated with the expression of *EDF1/2/3/4+SRDX* (Supplemental Fig. S6, D–G). This promotion further indicated that *EDF1/2/3/4+SRDX* functions downstream of *ETR1* and *EIN2* in regulating flower senescence/abscission.

35S:EDFs+SRDX Is Epistatic to *35S:FYF* in Regulating Flower Senescence and Abscission

To confirm the relationship between *EDF1/2/3/4* and *FYF*, transgenic plants containing both *35S:EDF1/2+SRDX* and *35S:FYF* were generated by genetic crossing. In the *35S:FYF* Arabidopsis, floral senescence/abscission was delayed until after position 9 (Fig. 3A; Chen et al., 2011). The phenotype of *35S:FYF/35S:EDF1/2+SRDX* resembled that of the *35S:EDF1/2+SRDX* plants (Fig. 3, B and C); they displayed early senescence/abscission of the perianth organs (positions before 3; Fig. 3, D and E), which was earlier than that in wild-type flowers (position 5; Fig. 1A). This promotion indicated that *35S:EDF1/2+SRDX* is epistatic to *35S:FYF* in regulating flower senescence/ abscission in the ethylene-insensitive response.

35S:FYF Significantly Suppressed the GUS Activity in *EDFs:GUS* Plants

To clearly show that the *FYF* negatively regulated the expression of the *EDFs* during flower development, transgenic plants containing both *EDF1/2/3/4: GUS* and *35S:FYF* were generated. The result clearly indicated that a significant reduction in the expression of GUS was observed in *EDF1/2/3/4:GUS/35S:FYF* plants. In contrast with *EDF1:GUS* flowers, in which strong GUS staining was detected in the sepals and petals of mature flowers (Fig. 3, F and G), GUS activity was almost undetectable in the *EDF1:GUS/35S:FYF* flower buds and mature flowers (Fig. 3, H and I). Similarly, compared with the high GUS activity in the mature flowers of *EDF2:GUS* (Fig. 3, J and K), *EDF3: GUS* (Fig. 3, N and O), and *EDF4:GUS* (Fig. 3, R and S), GUS staining was undetected in the floral buds and

mature flowers of plants carrying *EDF2:GUS/35S:FYF* (Fig. 3, L and M), *EDF3:GUS/35S:FYF* (Fig. 3, P and Q), and *EDF4:GUS/35S:FYF* (Fig. 3, T and U). This result strongly indicated that *EDF1/2/3/4* was negatively regulated by *FYF* during flower development.

The Identification of *FYF*-Regulated Genes by a Microarray Analysis

To further identify the downstream genes regulated by *FYF*, *FYF* was fused to the glucocorticoid receptor (GR; *35S:FYF+GR*) and transformed into Arabidopsis. The *35S:FYF+GR* plants grew normally and were indistinguishable from wild-type plants without dexamethasone (DEX) treatment (Supplemental Fig. S7, A and B). Upon DEX treatment, the *35S:FYF+GR* plants flowered early (Supplemental Fig. S7A) and exhibited delayed flower senescence and abscission (Supplemental Fig. S7, C and D), similar to the *35S:FYF* plants (Chen et al., 2011). This result indicated that this inducible strategy can be successfully used to study the genes regulated by *FYF*.

Thus, we performed a microarray analysis using the RNA extracted from the flowers of DEX-treated (3 h) and untreated *35S:FYF+GR* Arabidopsis; 107 up-regulated (2-fold or greater) and 10 down-regulated (0.5-fold or less) genes with *P* values less than 0.05 were identified in the DEX-treated plants (Supplemental Tables S5 and S6). Among 107 up-regulated genes, five ERFs—*AtERF19* (At1g22810), *AtERF21* (At1g71450), *AtERF95* (At3g23220), *AtERF96* (At5g43410), and *AtERF98* (At3g23230)—were identified (Supplemental Fig. S8, A and B; Supplemental Table S5). Because *EDF1-4* was not detected in this array experiment, this indicated that these *EDFs* are likely the indirect targets for *FYF* gene.

The Analysis of *FUF1* Expression

The ERF gene *AtERF21* (At1g71450), termed *FUF1*, is up-regulated by *FYF* (Fig. 4A; Supplemental Table S5) and was further characterized. Additional analysis indicated that a CArG box was found in the promoter (position −240) of the *FUF1* gene. The FUF1 protein contains an ERF/AP2 domain, which is conserved among the ERF/AP2-related proteins (Supplemental Fig. S8A; Sakuma et al., 2002; Nakano et al., 2006). To investigate the expression pattern of the *FUF1* gene, an *FUF1:GUS* construct was generated and transformed

Figure 3. (*Continued.*)
of *35S:EDF1+SRDX* (B), *35S:EDF2+SRDX* (C), *35S:FYF/35S:EDF1+SRDX* (D), and *35S:FYF/35S:EDF2+SRDX* (E) plants. The perianth organs of the flowers in these four plants were completely senescent and abscised at positions 2 and 3. F to U, GUS staining was weak in the flower buds (fbs) and stronger in the mature flowers (mfs) of *EDF1:GUS* (F and G), *EDF2:GUS* (J and K), *EDF3:GUS* (N and O), and *EDF4:GUS* (R and S) Arabidopsis. GUS staining was undetectable in the fbs and mature mfs of *EDF1:GUS/35S:FYF* (H and I), *EDF2:GUS/35S:FYF* (L and M), *EDF3:GUS/35S:FYF* (P and Q), and *EDF4:GUS/35S:FYF* (T and U) Arabidopsis. G, I, K, M, O, Q, S, and U are stage 13 mature flowers from F, H, J, L, N, P, R, and T, respectively. s, Sepal. Bars = 2 mm (F, H, J, L, N, P, R, and T) and 1 mm (G, I, K, M, O, Q, S, and U).
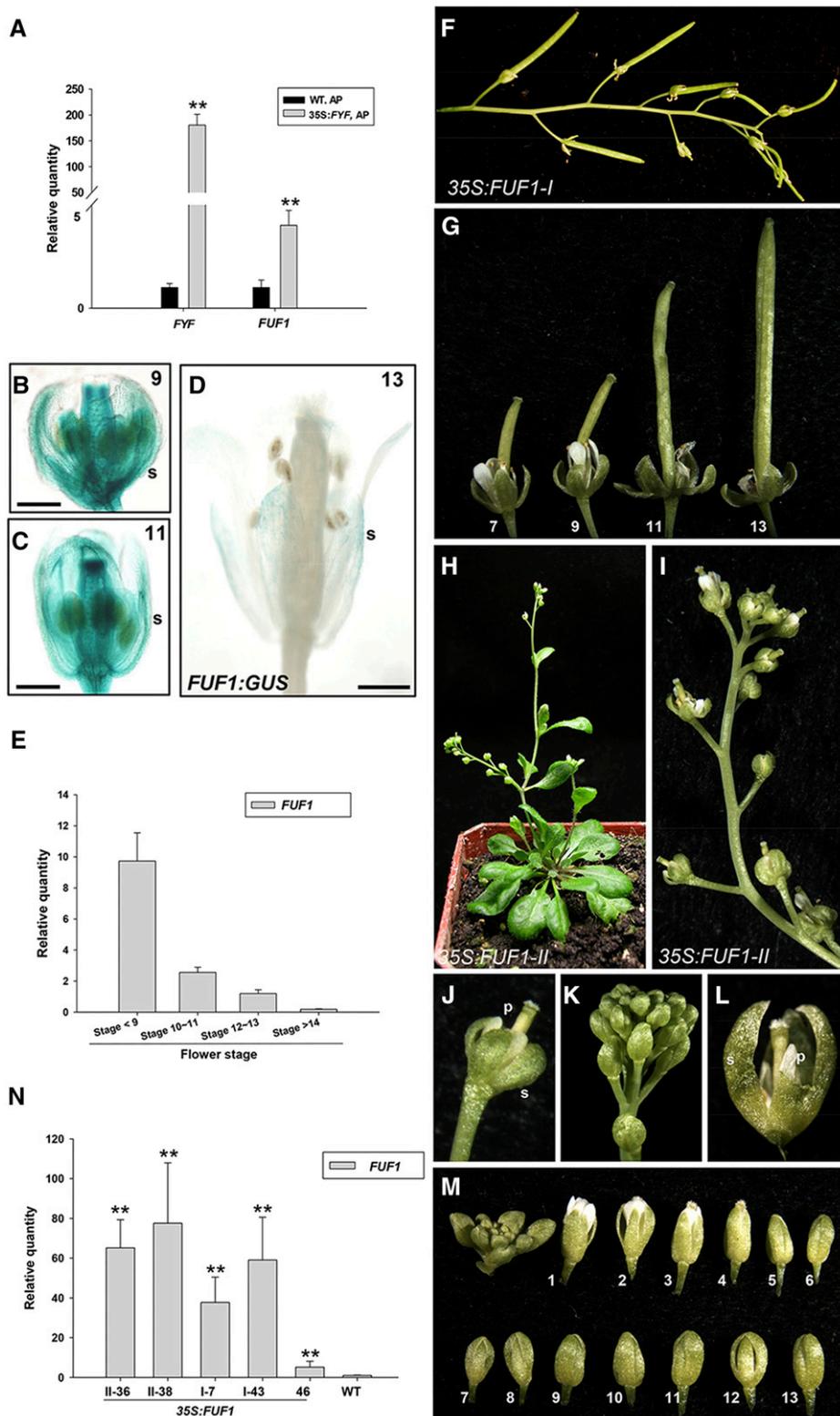
Figure 4. The ectopic expression of *FUF1* delays flower senescence and abscission. A, The expression levels of *FYF* and *FUF1* in flowers after stage 12 and pollination (AP) in wild-type (WT) and *35S:FYF* plants as determined by real-time quantitative RT-PCR. **, Significant difference from the wild-type value ($P \leq 0.01$). B and C, GUS staining was strong in the flower buds at stages 9 (B) and 11 (C) of *FUF1:GUS* Arabidopsis. s, Sepal. Bars = 0.5 mm (B), 1 mm (C). D, The GUS staining decreased in the stage 13 mature flowers of *FUF1:GUS* Arabidopsis. Bar = 1 mm. E, The detection of *FUF1* expression in wild-type flowers at four different developmental stages (<9, 10–11, 12–13, and >14). The mRNA levels were determined by real-time quantitative PCR.

into Arabidopsis. Similar to the GUS staining observed in *FYF:GUS* flowers (Supplemental Fig. S2), strong GUS staining was detected in sepals and petals of the flower buds and young flowers (Fig. 4, B and C) and significantly decreased in mature flowers after stage 13 of *FUF1:GUS* plants (Fig. 4D). When *FUF1* expression was further analyzed in flowers at different developmental stages, significantly higher *FUF1* expression was observed during early flower development (before stage 9) than during late developmental stages (after stage 12; Fig. 4E). These results indicate that the spatial and temporal expression pattern of *FUF1* is similar to that for *FYF* during flower development.

The Ectopic Expression of *FUF1* Delays Flower Senescence and Abscission in Transgenic Arabidopsis Plants

To investigate the function of *FUF1*, *35S:FUF1* was transformed into Arabidopsis; 80 of 200 *35S:FUF1* plants showed delayed flower senescence/abscission. These plants were divided into two classes based on the degree of phenotypic alteration.

In type I plants, the delay of senescence/abscission of the perianth (Fig. 4, F and G) was very similar to that observed in *35S:FYF* flowers (Fig. 3A; Chen et al., 2011). The perianth organs of these *35S:FUF1* transgenic flowers did not senesce and remained attached at the bases of the siliques for longer than position 13 (Fig. 4, F and G). Furthermore, the elongation of the siliques and the maturation of the seeds in these type I plants (Fig. 4, F and G) were normal, such as in *35S:FYF* plants. In type II plants, the delay of senescence/abscission of the perianths (Fig. 4, H–M) was enhanced compared with type I and *35S:FYF* flowers. These type II flowers produced short sepals and petals (Fig. 4, I and J), failed to open (Fig. 4, K–M) during almost the entire flower development, and did not senesce for longer than position 13 (Fig. 4, I and M). When these flowers were opened manually, we observed that the petals and stamens had failed to elongate (Fig. 4L). Interestingly, the enhancement of the delay in senescence/abscission of the perianths and the formation of the short sepals and petals in these type II flowers were similar to the phenotypes observed in the severe *35S:FYF+SRDX* flowers (Chen et al., 2011). As shown in Figure 4N, relatively

higher *FUF1* expression was observed in type II plants compared with type I plants.

The Formation of AZ Is Deficient in *35S:FUF1* Flowers

A break-strength meter was used to quantitatively measure the force required to remove the sepals from the plant as described previously (Chen et al., 2011). As shown in Figure 5A, we can only analyze the break strength of wild-type sepals at position 3. In contrast, the break strength of type I *35S:FUF1* sepals could be detected in the flowers at position 18 (Fig. 5A). In type II *35S:FUF1* plants, the sepals also could be detected in all nine flowers in the inflorescence (Fig. 5B).

Scanning electron microscopy (SEM) was used to further examine whether a normal sepal AZ developed in the *35S:FUF1* flowers. Upon sepal removal at position 2 in wild-type and *35S:FUF1* flowers, broken cells were observed at the fracture planes of the sepal AZs (Fig. 5C, 2 and 5D, 2). At position 4, wild-type AZ cells began to display an initial rounded appearance without any obviously ruptured cells (Fig. 5C, 4). At position 8, wild-type AZ cells were fully round (Fig. 5C, 8). In contrast, the broken cells at the fracture plane could still be observed in the *35S:FUF1* flowers after the sepal removal at positions 4 and 8 (Fig. 5D, 4 and 8). This pattern indicated that the timing of cell separation was significantly delayed in the AZ of the *35S:FUF1* flowers.

To further examine the deficiency of abscission in *35S:FUF1*, thin sections of embedded flowers were generated and analyzed. In the wild-type flower at position 4, small differentiated cells were clearly formed in the AZ of the sepals (Fig. 5E, 1 and 5E, 2). In contrast, the cells were not differentiated, and the AZ was not formed in the *35S:FUF1* sepal (Fig. 5E, 3 and 5E, 4). This result indicated that the deficiency of abscission in *35S:FUF1* was clearly caused by a deficiency or significant delay in floral AZ formation.

BOP1/2, *IDA*, *HAE*, *HSL2*, and *HWS* Expression Levels Are Down-Regulated in Plants Carrying *35S:FUF1*

BOP1 and *BOP2* are required for the formation of the floral AZ (McKim et al., 2008). The expression levels of *BOP1/2* in wild-type and *35S:FUF1* flowers

Figure 4. (*Continued.*)
F and G, An inflorescence (F) and flowers along the inflorescence (G) of a *35S:FUF1* type I plant. The perianth organs of the *35S:FUF1* flowers did not senesce and remained attached to the bases of the siliques after position 13. H and I, A 40-d-old *35S:FUF1* type II plant (H) and a close-up image of a type II inflorescence (I). The perianth organs of this *35S:FUF1* type II plant did not senesce and remained attached to the bases of the siliques in positions greater than 13. J, A close-up image of a *35S:FUF1* type II flower from I that contained short s and petal (p) and that did not senesce or abscise. K, A close-up image of the flowers in a *35S:FUF1* type II inflorescence. These flowers failed to open and did not senesce for a long period. L, Close-up image of a type II *35S:FUF1* flower from K that was manually opened. M, The flowers along an inflorescence of a *35S:FUF1* type II plant failed to open, and the perianth organs did not senesce or abscise even after position 13. N, The detection of *FUF1* expression in *35S:FUF1* plants. The mRNA levels were determined by real-time quantitative PCR. Total RNA was isolated from one wild-type Col-0 plant, two type II plants (36 and 38), two type I plants (7 and 43), and one *35S:FUF1* plant (46) with a wild-type-like phenotype. Expression statistical analysis was measured by Student's *t* test (each $n = 3$). **, Significant difference from the wild-type value ($P \leq 0.01$).
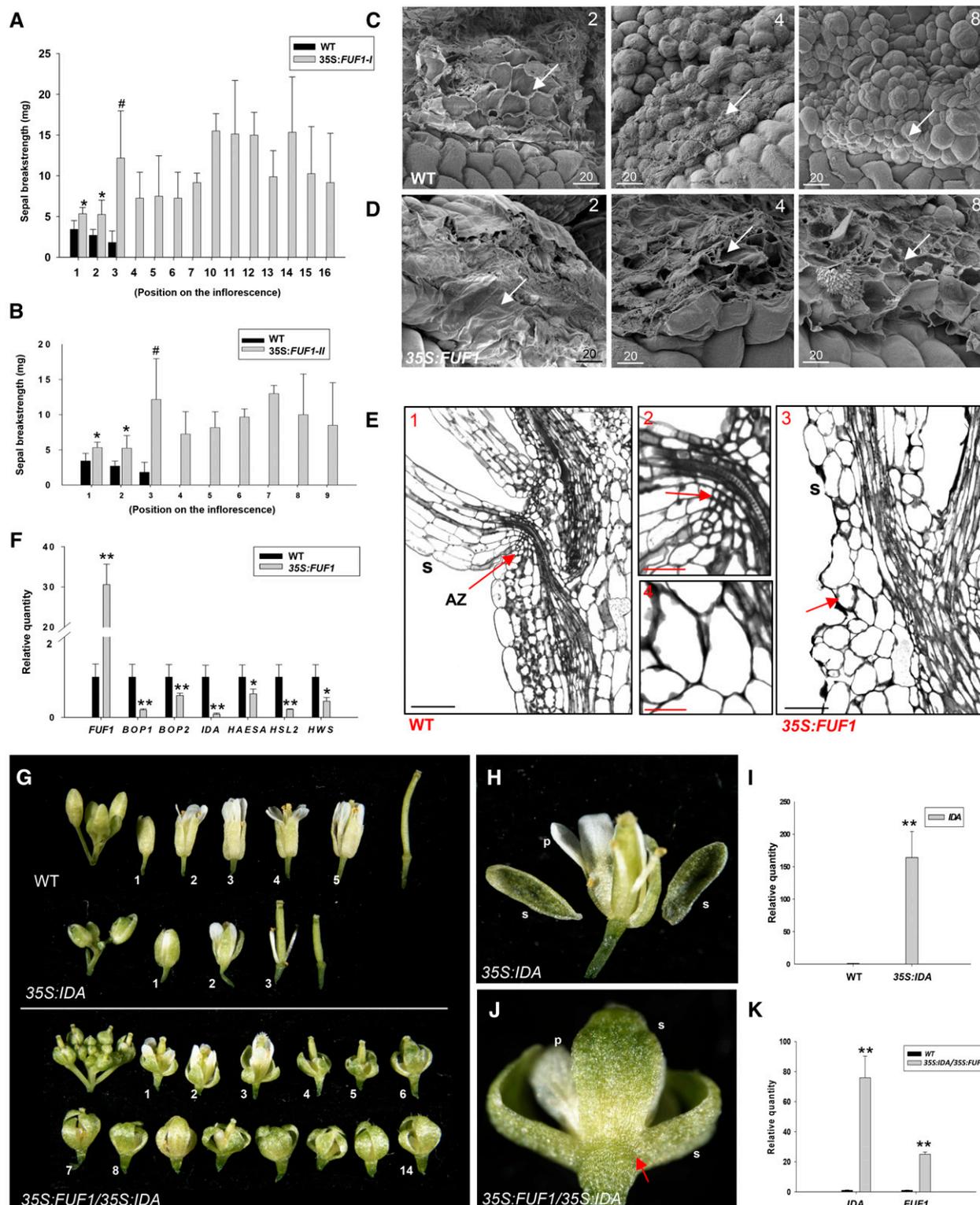
Figure 5. The detection sepal break strength, the morphology of the AZs, and the gene expression for *35S:FUF1* plants as well as a phenotypic analysis of flower senescence and abscission in *35S:FUF1* plants ectopically expressing the *IDA* gene. A and B, Sepal break strength measured from positions 1 to 3 for wild-type (WT), positions 1 to 16 for *35S:FUF1* type I (A), and positions 1 to 9 for *35S:FUF1* type II (B) plants along the inflorescence. C and D, SEM image of Arabidopsis sepal AZs (arrows) in wild-type (C) and *35S:FUF1* (D) flowers at positions 2, 4, and 8. Bars = 20 μm. E, Thin sections of embedded flowers at position 4 for wild-type flower (E, 1 and 2) and *35S:FUF1* (E, 3 and 4). E, 2 and 4 are close-up images of E, 1 and 3, respectively. Arrows indicate the positions of the AZ of the sepals (s). The small AZ cells were not formed in the *35S:FUF1* s. Bars = 25 μm (E, 1),

were analyzed. The results indicated that *BOP1/2* was significantly down-regulated in the *35S:FUF1* flowers compared with the wild-type flowers (Fig. 5F). Thus, *FUF1* likely functions upstream of *BOP1/2* to negatively regulate AZ formation and flower abscission.

IDA has been proposed to interact with the receptor-like kinases HAESA and HSL2 to regulate flower organ abscission (Cho et al., 2008; Stenvik et al., 2008). A mutation in *HWS* also displays defects in organ abscission (Gonzalez-Carranza et al., 2007b). We thus analyzed the expression levels of *IDA/HAESA/HSL2/HWS* in wild-type and *35S:FUF1* flowers. These four genes were all significantly down-regulated in the *35S:FUF1* flowers compared with the wild-type flowers (Fig. 5F). Thus, *FUF1* likely negatively regulates *IDA/HAESA/HSL2/HWS* to control flower abscission.

35S:FUF1 Delays Flower Senescence and Abscission in Plants Carrying *35S:IDA*

To further explore the relation between *FUF1* and *IDA*, the *35S:FUF1* construct was transformed into plants carrying the *35S:IDA* construct. The abscission of flower organs was clearly promoted at positions 2 and 3 in the *35S:IDA* transgenic plant (Fig. 5, G and H). This early abscission correlated with high levels of *IDA* gene expression in the transgenic plant (Fig. 5I). In contrast, *35S:IDA/35S:FUF1* double transgenic plants, which highly expressed both *IDA* and *FUF1* (Fig. 5K), displayed a significant delay in flower organ abscission (Fig. 5, G and J), similar to that observed in *35S:FUF1* transgenic plants. This result indicated that the failure of AZ formation in *35S:FUF1* flowers prevented the abscission of the flower organs, even with the ectopic expression downstream of abscission-associated genes, such as *IDA*.

35S:FUF1 Arabidopsis Plants Are Insensitive to Ethylene Treatment

In the presence of air, the leaves remained green (Fig. 6, C and D, left), and the perianth organs remained attached to the flowers until position 5 in wild-type plants (Fig. 6A, upper) but did not senesce or abscise in the *35S:FUF1* transgenic plants (Fig. 6B, upper). When ethylene was added to wild-type plants, the

leaves senesced (Fig. 6C, right), and the perianth organs abscised early (at position 2; Fig. 6A, lower). In contrast, in the presence of ethylene, the leaves of the *35S:FUF1* transgenic plants remained green (Fig. 6D, right; Supplemental Fig. S9), and the perianth organs were turgid and remained on the flowers (Fig. 6B, lower). These results indicated that the delay of senescence and abscission of the flower organs in the *35S:FUF1* Arabidopsis was unaffected by the ethylene treatment.

35S:FUF1 Enhances the Delay of Flower Senescence and Abscission in *etr1*, *ein2*, and *ctr1* Mutants

To further confirm the relation between *FUF1* and the ethylene signaling pathway, the *35S:FUF1* construct was transformed into the Arabidopsis mutants *etr1*, *ein2*, and *ctr1*. The phenotypes of the *35S:FUF1/etr1-1* and *35S:FUF1/ein2-1* plants resembled the phenotype of the *35S:FUF1* plants; these plants displayed delayed senescence/abscission of the perianth organs at positions greater than 9 for *35S:FUF1/etr1-1* (Fig. 6, E and F) or greater than 18 for *35S:FUF1/ein2-1* (Fig. 6, G and H). This was later than that in the untransformed *etr1-1* and *ein2-1* mutants, which abscised at positions 7 and 8, respectively (Fig. 6, E and G, center). This delay indicated that *35S:FUF1* functions downstream of *ETR1* and *EIN2* in the ethylene-insensitive response.

Mutations in the *CTR1* gene caused a constitutive ethylene response and early senescence/abscission of the flowers (Fig. 6, J and L, upper; Kieber et al., 1993; Huang et al., 2003). The size of the *35S:FUF1/ctr1-1* plants (Fig. 6I, center) was also reduced and resembled that of the untransformed *ctr1-1* mutants (Fig. 6I, left). However, the senescence/abscission of the perianth organs was delayed in these plants (Fig. 6, K and L, lower), which was observed for the *35S:FUF1* plants. This delay indicates that *35S:FUF1* functions downstream of *CTR1* and was epistatic to *ctr1* mutants in regulating flower senescence/abscission.

FUF1 Inhibits *EDF* Genes in the Ethylene Response

To further investigate the involvement of the *FUF1* gene in ethylene signaling, the expression levels of *EDF*s were analyzed in *35S:FUF1* plants. *EDF1*, *EDF3*,

Figure 5. (*Continued.*)
10 μm (E, 2), 50 μm (E, 3), and 20 μm (E, 4). F, The expression levels for *FUF1*, *BOP1*, *BOP2*, *IDA*, *HAESA*, *HSL2*, and *HWS* in wild-type and *35S:FUF1* flowers using real-time quantitative RT-PCR. G, The flowers along an inflorescence of the wild-type, *35S:IDA*, and *35S:FUF1/35S:IDA* plants. The perianth organs of the flowers in *35S:IDA* plants were abscised at positions 2 and 3. The perianth organs did not senesce and abscised after position 14 for *35S:FUF1/35S:IDA*. The numbers indicate the positions of the flowers. H, Close-up view of a flower at position 2 for the *35S:IDA* plant from G. The s and petals (p) were abscised and easily dropped by a gentle touch. I, The expression levels for *IDA* in wild-type and *35S:IDA* flowers using real-time quantitative RT-PCR. J, Close-up view of a flower at position 14 for the *35S:FUF1/35S:IDA* plant from G. The s and p were not abscised and remained firmly attached to the base of the flowers (arrow). K, The expression levels for *IDA* and *FUF1* in wild-type and *35S:FUF1/35S:IDA* flowers using real-time quantitative RT-PCR. Expression statistical analysis was measured by Student's *t* test (each *n* = 3). Symbols in A, B, F, I, and K indicate a significant difference from the wild type value. *, $P \leq 0.05$; **, $P \leq 0.01$; #, $0.1 \leq P \leq 0.05$.
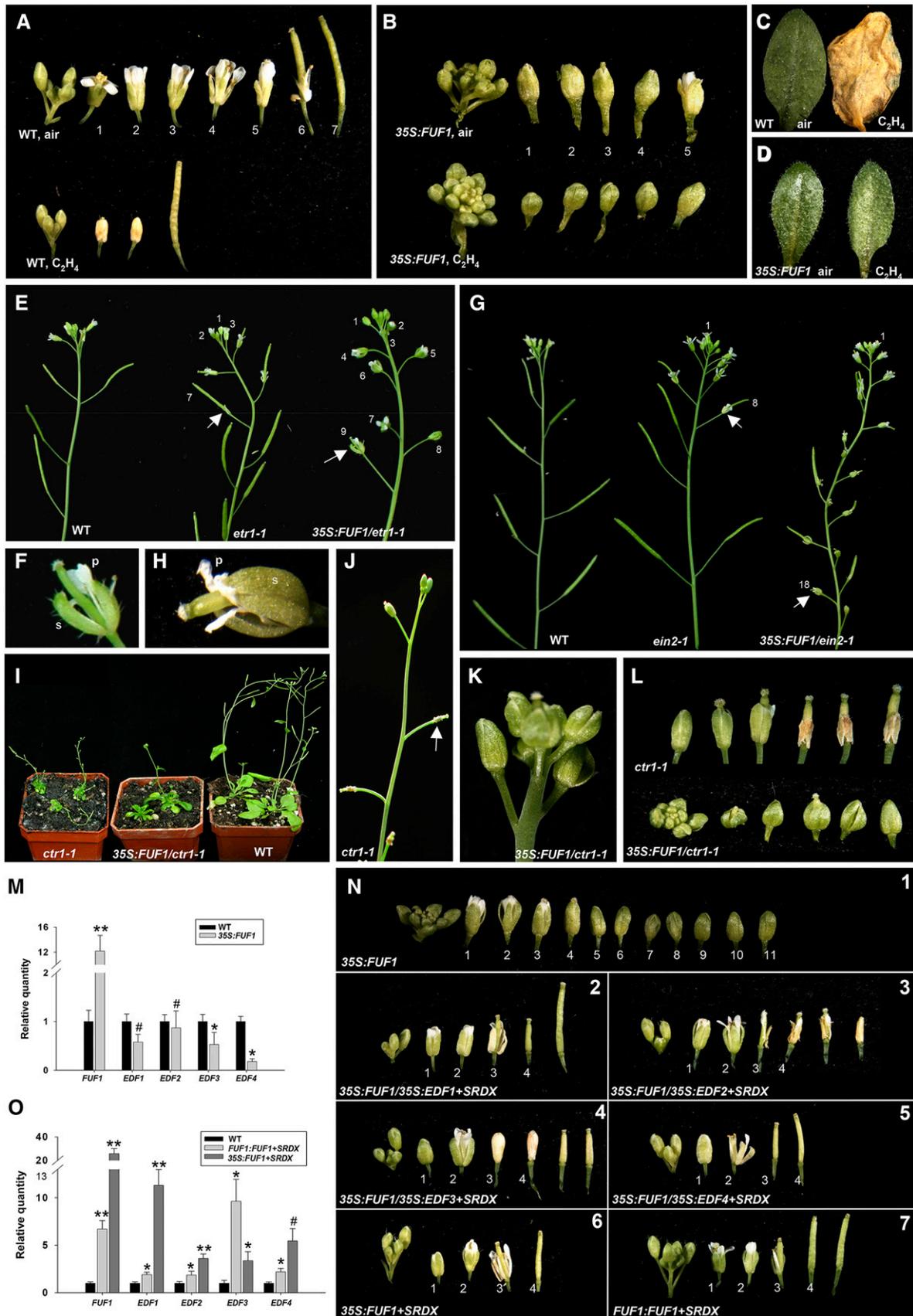
Figure 6. An analysis of the effect of ethylene on *35S:FUF1* Arabidopsis and a phenotypic analysis of flower senescence and abscission in *etr1-1*, *ein2-1*, *ctr1-1*, and *35S:EDFs+SRDX* plants ectopically expressing the *FUF1* gene as well as in *FUF1+SRDX* plants. A and B, A comparison of wild-type (WT; A) and *35S:FUF1* (B) flowers exposed to either air (upper) or ethylene (lower).

and *EDF4* were clearly down-regulated in the *35S:FUF1* plants (Fig. 6M). These results indicated that the delayed flower senescence/abscission of the *35S:FUF1* plants was because of the *FUF1*-mediated inhibition of the downstream genes in the ethylene response.

To further confirm the relationship between *FUF1* and the *EDFs*, transgenic plants containing both *35S:EDF1/2/3/4+SRDX* and *35S:FUF1* were generated by genetic crossing. Floral senescence/abscission was delayed to later than position 10 (Fig. 6N, 1) in *35S:FUF1* plants. By contrast, *35S:FUF1/35S:EDF1/2/3/4+SRDX* plants displayed early senescence/abscission of the perianth organs at positions less than 3 (Fig. 6N, 2–6N, 5), which is the same phenotype as the *35S:EDF1/2/3/4+SRDX* plants (Fig. 1F). This phenotype confirmed that *EDF1/2/3/4+SRDX* functions downstream of *FUF1* in the ethylene response.

Flower Senescence and Abscission Are Significantly Promoted, and *EDFs* Are Up-Regulated in the *FUF1+SRDX* Transgenic Dominant-Negative Plants

To determine if any phenotypes were produced in an *FUF1* loss-of-function mutant, an *FUF1* transfer DNA insertion line, SALK_136922 (containing an insertion in the 5′-untranslated region [UTR]), was analyzed. The flower organ senescence/abscission occurred similarly in the SALK_136922 flowers compared with the wild-type flowers (Supplemental Fig. S10). This indicated a possible functional redundancy for *FUF1* and other unknown genes. To examine this assumption, a strategy to generate transgenic dominant loss-of-function mutant plants was performed by fusing the conserved SRDX-suppressing motif (Chen et al., 2011) to FUF1 (*FUF1+SRDX*). If *FUF1* functions as an activator, we expect that *35S:FUF1+SRDX* should convert *FUF1* into a repressor and cause a dominant-negative effect, resulting in the opposite phenotype to that observed in the *35S:FUF1* plants.

In total, 41 of 100 independent *35S:FUF1+SRDX* kanamycin-resistant Arabidopsis plants exhibited an abnormal phenotype of significantly early flower senescence/abscission. Unlike the perianths of the *35S:FUF1* flowers, which began to senesce and abscise in a turgid state at positions later than 10 (Fig. 6N, 1), early senescence/abscission was observed in the *35S:FUF1+SRDX* plants at positions before 3 (Fig. 6N, 6).

We further expressed *FUF1+SRDX* under its own promoter (*FUF1:FUF1+SRDX*) through the transactivation system (Hsu, 2012). The resulting plants showed similar early senescence/abscission of the perianths (Fig. 6N, 7). These results indicated that the *FUF1* gene encodes a transcriptional activator; *35S:FUF1+SRDX* and *FUF1:FUF1+SRDX* result in the opposite phenotype of that observed in the *35S:FUF1* plants. In contrast to the gene expression detected in the *35S:FUF1* plants, the expression levels of *EDF1/2/3/4* were clearly up-regulated in the *35S:FUF1+SRDX* and *FUF1:FUF1+SRDX* plants (Fig. 6O).

DISCUSSION

EDFs Function as Downstream Genes in the Ethylene Response in Controlling Flower Senescence and Abscission

Our previous results suggested that *EDFs* may function as downstream genes in the ethylene response and may be suppressed by *FYF* in the control of flower senescence/abscission (Chen et al., 2011). In this study, we provide evidence to support this assumption through a functional analysis of the *EDF1/2/3/4* genes.

First, weak *EDF1/2/3/4* expression was detected in the young flower buds and increased significantly in mature flowers. This pattern was opposite of that for *FYF* (Chen et al., 2011) and reveals opposite roles for *EDFs* and *FYF*. Second, *35S:EDFs* and *35S:EDFs+SRDX* promoted flower senescence/abscission in transgenic Arabidopsis plants by activating *SAG12* and the PCD-associated genes *AtMCs* and *VPEs*. This result indicated that *EDF1/2/3/4* functions as a repressor to promote senescence/abscission in contrast to *FYF*.

Figure 6. (*Continued.*)
C and D, A rosette leaf from a wild-type plant (C, right) was senescent; however, a leaf from a *35S:FUF1* plant (D, right) remained green after ethylene treatment. E, The inflorescences of wild-type (left), *etr1-1* (center), and *35S:FUF1/etr1-1* (right) plants. The floral organs (arrows) remained on the flowers and siliques of the *etr1-1* and *35S:FUF1/etr1-1* plants until approximately positions 7 and 9, respectively. F, Close-up view of the flower at position 9 for the *35S:FUF1/etr1-1* plant from E. p, Petal; s, sepal. G, The inflorescences of wild-type (left), *ein2-1* (center), and *35S:FUF1/ein2-1* (right) plants. The floral organs (arrows) remained on the flowers and siliques of the *ein2-1* and *35S:FUF1/ein2-1* plants until approximately positions 8 and 18, respectively. H, Close-up view of the flower at position 18 for the *35S:FUF1/ein2-1* plant from G. I, Adult *ctr1-1* (left), *35S:FUF1/ctr1-1* (center), and wild-type (right) plants. J, An inflorescence of a *ctr1-1* mutant. The floral organs senesced (arrow) at an early stage. K, An inflorescence of a *35S:FUF1/ctr1-1* plant. The floral organs were green and remained on the flowers. L, The flowers along inflorescences of *ctr1-1* (upper) and *35S:FUF1/ctr1-1* (lower) plants. The perianths of the *35S:FUF1/ctr1-1* flowers were green and displayed no signs of senescence or abscission at the late stages. M, The expression levels of *FUF1*, *EDF1*, *EDF2*, *EDF3*, and *EDF4* in wild-type and *35S:FUF1* flowers using real-time quantitative RT-PCR. N, The flowers along the inflorescences of plants carrying *35S:FUF1* (type II plant; N, 1), *35S:FUF1/35S:EDF1+SRDX* (N, 2), *35S:FUF1/35S:EDF2+SRDX* (N, 3), *35S:FUF1/35S: EDF3+SRDX* (N, 4), *35S:FUF1/35S:EDF4+SRDX* (N, 5), *35S:FUF1+SRDX* (N, 6), and *FUF1:FUF1+SRDX* (N, 7). O, The expression levels of *FUF1*, *EDF1*, *EDF2*, *EDF3*, and *EDF4* in wild-type, *35S:FUF1+SRDX*, and *FUF1:FUF1+SRDX* flowers using real-time quantitative RT-PCR. Expression statistical analysis was measured by Student's *t* test (each *n* = 3). The asterisks in M and O indicate a significant difference from the wild-type value. *, $P \leq 0.05$; **, $P \leq 0.01$; #, $0.1 \leq P \leq 0.05$.
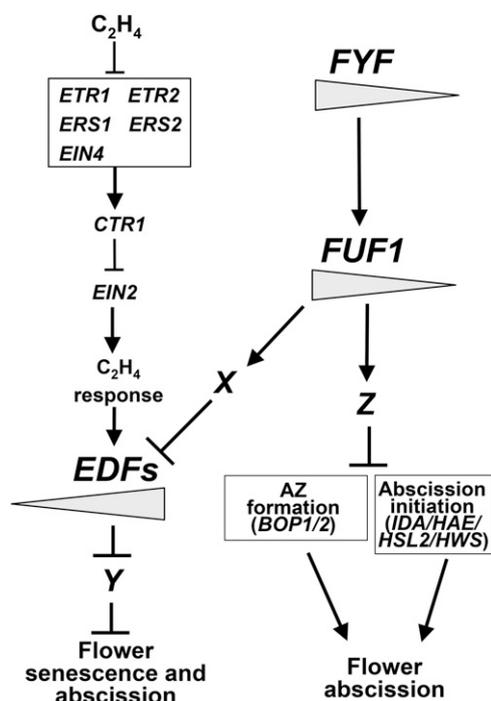
Figure 7. A model for the function of *FYF* and *FUF1* genes in regulating flower senescence and abscission. In wild-type flowers, *FYF* negatively regulates the ethylene signaling pathway by activating (→) the expression of *FUF1*. In this pathway, *FUF1* activates (→) an X gene, which negatively regulates (line with bar) the *EDF1/2/3/4* downstream genes of the ethylene signaling pathway. *EDF1/2/3/4* promotes the senescence/abscission by suppressing (line with bar) a Y gene that functions to suppress (line with bar) the senescence/abscission. The suppression of *EDF1/2/3/4* before pollination results in the repression of senescence/abscission. This pathway also regulates abscission by activating (→) a Z gene that suppresses (line with bar) the expression of *BOP1* and *BOP2*, which regulate the formation of the AZ and the expression of genes, such as *IDA/HAESA/HSL2/HWS*, that regulate the initiation of abscission. The ectopic expression of *FYF* or *FUF1* suppressed *EDF1/2/3/4*, *BOP1/2*, and *IDA/HAESA/HSL2/HWS* and caused the inhibition of senescence/abscission during all stages of flower development. The gradient of *FYF* and *FUF1* activity is illustrated as the gradual reduction in the size of the gray bar during flower maturation. In contrast, the gradient of *EDF1/2/3/4* activity is illustrated as the gradual increase in the size of the gray bar during flower maturation.

Third, *35S:EDF*s+*SRDX* is epistatic to *35S:FYF*. Fourth, GUS activity in *EDFs:GUS* plants was significantly suppressed by *35S:FYF*. These results support the conclusion that *EDF1/2/3/4* functions downstream of *FYF* and that the expression before pollination is suppressed by *FYF*. This suppression prevents the flowers from senescing and abscising. The decrease in *FYF* expression after pollination activates *EDF1/2/3/4* and the ethylene signaling pathway, resulting in the senescence/abscission of the flowers.

The involvement of *EDF1/2/3/4* in the ethylene signaling pathway was further supported by the analysis of the *etr1* and *ein2* mutants that ectopically expressed *EDFs*+*SRDX*. These plants displayed early senescence/abscission of the perianth organs, which was observed in

35S:EDFs+*SRDX* plants, suggesting that *35S:EDFs*+*SRDX* is epistatic to both *etr1* and *ein2* mutants in the ethylene-insensitive response. This assumption was further supported by the result that EIN3 binds to the promoters of all four *EDF*s (Chang et al., 2013). Thus, the hypotheses that *EDF*s are downstream genes in the ethylene response and suppressed by *FYF* in controlling flower senescence and abscission were confirmed. Interestingly, although *EDF*s caused very similar effect on the promotion of the flower senescence/abscission, it seems that *EDF2* has a relatively stronger effect than *EDF1*, *EDF3*, and *EDF4* (Supplemental Tables S1–S4). This result may reflect the small functional difference among the genes with redundant activity.

FUF1 Acts as an Activator Downstream of *FYF* in Controlling Flower Organ Senescence and Abscission

FUF1, which up-regulated by *FYF*, was hypothesized to be related to the regulation of senescence/abscission, and this assumption was supported by three lines of evidence. The first line of evidence originates from the significant delay in floral organ senescence/abscission observed in the *35S:FUF1* plants, similar to the delay observed in the *35S:FYF* plants. The second line of evidence originates from the expression pattern of the *FUF1* gene during flower development. Similar to the GUS expression pattern in *FYF:GUS* Arabidopsis, strong GUS activity was detected in the young flower buds; however, this staining significantly decreased after anthesis in *FUF1:GUS* plants. The third line of evidence originates from the significant promotion of flower organ senescence/abscission in the *35S:FUF1*+*SRDX* and *FUF1:FUF1*+*SRDX* dominant-negative plants in contrast to the phenotype of the *35S:FUF1* plants. These results indicated that *FUF1* functions as a transcriptional activator to prevent the senescence/abscission of flowers during the early stages of floral development. This inhibition extends to late flower development in the *35S:FUF1* plants and results in the delay of flower senescence and abscission. In contrast, this inhibition was reversed in the *FUF1*+*SRDX* plants, which exhibited early senescence/abscission.

FUF1 Controls Senescence and Abscission through Inhibiting the *EDF*s, Which Are Downstream Genes in the Ethylene Response

Similar to the plants carrying *35S:FYF*, the floral senescence/abscission of the *35S:FUF1* plants was also insensitive to ethylene treatment, further supporting the idea that *FUF1* acts downstream of *FYF* to control floral senescence/abscission by suppressing the ethylene response.

This hypothesis was supported by the analysis of the *etr1*, *ein2*, and *ctr1* mutants ectopically expressing *FUF1*. The results indicated that, similar to that in plants carrying *35S:FUF1*, enhanced delay of the

senescence/abscission of the perianth organs was observed in the *35S:FUF1/etr1-1* and *35S:FUF1/ein2-1* plants, suggesting that *35S:FUF1* is epistatic to both *etr1* and *ein2* mutants in the ethylene-insensitive response. Furthermore, the senescence/abscission of the perianth organs was significantly delayed in the constitutive ethylene response mutant *ctr1-1* ectopically expressing *FUF1* (*35S:FUF1/ctr1-1*). This result suggests that *35S:FUF1* repressed the genes that function downstream of *CTR1* in controlling the constitutive ethylene response and regulating flower senescence/abscission. This assumption was supported by the observed down-regulation of *EDFs* in *35S:FUF1* plants. Conversely, the expression level of *EDF1/2/3/4* was up-regulated in the *35S:FUF1+SRDX* and *FUF1:FUF1+SRDX* dominant-negative plants, in which senescence/abscission was greatly promoted. In addition, *35S:EDFs+SRDX* is epistatic to *35S:FUF1*. These results support the conclusions that *EDF1/2/3/4* functions downstream of *FUF1* and that the expression before pollination is suppressed by *FUF1*.

The hypothesis that *FUF1* functions downstream of *FYF* to regulate the ethylene response during plant growth and development was further supported by two additional results. First, neither *35S:FUF1* nor *35S:FYF* rescued the reduction in plant size in the *ctr1* mutant. This result suggests that *FYF* and *FUF1* are involved in the ethylene response pathway that controls flower senescence and abscission but not the other ethylene response pathways that control plant growth and development, including plant size (Chen et al., 2011). Second, as observed for *35S:FYF*, the senescence of the *35S:FUF1* leaves was insensitive to ethylene treatment, supporting the notion that the *FYF/FUF1* pathway may also control leaf senescence in a similar manner to its control of flower senescence by repressing the ethylene response.

FUF1 Controls Abscission through the Down-Regulation of *BOP1, BOP2, IDA, HAESA, HSL2,* and *HWS*

In addition to regulating ethylene-responsive genes, a clear down-regulation of *BOP1/2* expression was observed in the *35S:FUF1* flowers. Because the *BOP1/2* genes function in the control of floral AZ formation (McKim et al., 2008), *BOP1/2* suppression by *FUF1* may block abscission. This hypothesis was supported by the lack or significant delay of the AZ formation in the *35S:FUF1* flowers, which was determined by SEM examination of a thin section of the *35S:FUF1* sepals. Thus, *FUF1* likely suppresses the abscission of the floral organs primarily through the down-regulation of *BOP1/2* and the repression of the AZ formation. In addition to *BOP1/2*, the expression of the abscission-associated genes *IDA/HAESA/HSL2/HWS*, which regulate the abscission initiation of the floral organs, was also down-regulated in the *35S:FUF1* flowers. *FUF1* may be directly responsible for the suppression of *IDA/HAESA/HSL2/HWS* expression. Alternatively, if the ectopic expression of *FUF1* caused deficient AZ

formation, then this result might have a consequence on the down-regulation of *IDA/HAESA/HSL2/HWS* expression. To distinguish these two possibilities, the *35S:FUF1/35S:IDA* double transgenic plants were generated, and the phenotype was analyzed. The result indicated that *35S:FUF1/35S:IDA* plants showed the similar *35S:FUF1* phenotype, and thus, it supports the latter assumption. This conclusion is further supported by a previous study that showed that *35S:IDA* phenotype was also suppressed by *bop1/bop2* double mutants (McKim et al., 2008). It has been shown that *35S:IDA bop1/bop2* plants clearly lack floral organ abscission similar to *bop1/bop2* and our *35S:FUF1/35S:IDA* plants. Thus, the failure of AZ formation because of the suppression of *BOP1/2* expression in *35S:FUF1* flowers prevented the abscission of the flower organs, even with the ectopic expression downstream of abscission-associated genes, such as *IDA*.

A model depicting the possible roles of the *FYF* and *FUF1* genes in regulating genes associated with senescence, abscission, and ethylene signaling is illustrated in Figure 7. Thus, this report presents data that extend the knowledge of the genes in a pathway regulated by the *FYF* gene, which controls flower senescence and abscission.

MATERIALS AND METHODS

Plant Materials and Plant Transformation

The *etr1-1* (CS237) Arabidopsis (*Arabidopsis thaliana*) seeds were obtained from Long-Chi Wang (Biotechnology Center, National Chung Hsing University). The *ein2-1* (CS3071) and *ctr1-1* (CS8057) mutant Arabidopsis seeds were obtained from the Arabidopsis Biological Resource Center. Seeds for Arabidopsis were germinated and grown as described previously (Chang et al., 2010). Arabidopsis seeds were sterilized and placed on agar plates containing one-half-strength Murashige and Skoog medium (Murashige and Skoog, 1962) at 4°C for 2 d. Before being transplanted into soil, the seedlings were grown in growth chambers with the light intensity at 150 μE m^{-2} s^{-1} under long-day conditions (16-h-light/8-h-dark cycle) at 22°C for 10 d. A floral dip method as described elsewhere (Clough and Bent, 1998) was used to introduce constructs in the *Agrobacterium tumefaciens* strain GV3101 into Arabidopsis plants. Transformants that survived in medium containing kanamycin (50 μg mL^{-1}) were further verified by PCR and reverse transcription (RT)-PCR analyses. More than 10 transgenic plants with the similar altered phenotype for each construct were phenotype analyzed to confirm the function of the transgene and avoid the effect that the 35S promoter may switch on the downstream gene in different tissues and with different timing to the native promoter in transgenic plants. To generate *35S:FUF1/ctr1-1* Arabidopsis, homozygous *35S:FUF1* plants were crossed with the *ctr1-1* mutant in the Columbia-0 (Col-0) background, and F1 plants resistant to kanamycin were selected to generate the F2 generation. One-quarter of the F2 plants that were resistant to kanamycin were *35S:FUF1/ctr1-1* and selected for additional analysis.

Cloning of the Complementary DNAs for *EDF1/2/3/4* from Arabidopsis

For 35S:*EDF1/2/3/4* constructs, the complementary DNAs (cDNAs) for *EDF1* (At1g25560), *EDF2* (At1g68840), *EDF3* (At3g25730), and *EDF4* (At1g13260) were obtained by PCR amplification and sequence confirmed. The primers contained the *Xba*I and *Kpn*I recognition sites for *EDF1/2/4* and the *Bam*HI and *Kpn*I recognition sites for *EDF3* to facilitate the cloning of the cDNAs. The *Xba*I-*Kpn*I or *Bam*HI-*Kpn*I fragment containing the cDNA was cloned into the binary vector pEpyon-32K (Chen et al., 2011) under the control of the *Cauliflower mosaic virus* (CaMV) 35S promoter and used for plant transformation. Sequences for the primers are listed in Supplemental Table S7.

Cloning of the cDNA for *FUF1* from Arabidopsis

For the *35S:FUF1* construct, the cDNA for *FUF1* (At1g71450) was obtained by PCR amplification and sequence confirmed. The primers contained the *Xba*I and *Kpn*I recognition sites to facilitate the cloning of the cDNA. The *Xba*I-*Kpn*I fragment containing the cDNA was cloned into the binary vector pEpyon-12K (Chen et al., 2011) under the control of the CaMV 35S promoter and used for plant transformation. Sequences for the primers are listed in Supplemental Table S7.

Cloning of the Promoter DNA Fragment from Arabidopsis

For the EDF1/2/3/4:GUS constructs, the promoter regions that included the 5′-UTR for EDF1 (2.12 kb), EDF2 (2.07 kb), EDF3 (2.03 kb), and EDF4 (2.07 kb) were obtained by PCR amplification and sequence confirmed from the genomic DNA followed by cloning into the pGEM-T easy vector (Promega). These EDF1/2/3/4 promoter fragments were then subcloned into the linker region before the GUS coding region in the binary vector pEpyon01k (Peng et al., 2013). For the FUF1:GUS construct, the FUF1 promoter that included the 5′-UTR (2.46 kb) was obtained by PCR amplification from the genomic DNA; this was then cloned into the pGEM-T easy vector. The FUF1 promoter fragment was then subcloned into the linker region before the GUS coding region in the binary vector pEpyon01k. The sequences of the primers are listed in Supplemental Table S7.

Construction of the *35S:EDF1/2/3/4+SRDX* and *35S:FUF1+SRDX* Constructs

For the *35S:EDF1/2/3/4+SRDX* construct, the cDNAs for *EDF1/2/3/4* were obtained by PCR amplification and cloned into the pEpyon-3aK plasmid upstream of the SRDX (LDLDLELRLGFA*) sequence under the control of the CaMV 35S promoter as described previously (Chen et al., 2011). For the *35S:FUF1+SRDX* construct, the cDNA for *FUF1* was obtained by PCR amplification and cloned into the pEpyon-3aK in the same manner as *35S:EDF1/2/3/4+SRDX*. The sequences of the primers are listed in Supplemental Table S7.

Generation of the *FUF1:FUF1+SRDX* Construct

The transactivation system was used to generate the *FUF1:FUF1+SRDX* construct. The *FUF1+SRDX* fragment was obtained by PCR amplification and cloned into the effector line vector pEpyon-7aK downstream of the LexA operator that was used as the upstream activating sequence (Hsu, 2012). The *FUF1* promoter (2.46 kb) was cloned into the activator line vector pBroly-KXV upstream of the chimeric transcription factor LexA-VP16, which recognizes the LexA operator DNA sequence. These constructs (pEpyon-7aK and pBroly-KXV) were transformed into Arabidopsis plants separately. The transactivation line (*FUF1:FUF1+SRDX*) was obtained by crossing the effector line and the activator line.

GUS Staining and Microscopy

Histochemical staining was performed under standard methods described previously (Jefferson et al., 1987; Chou et al., 2001). SEM was performed according to the methods by Tzeng and Yang (2001), Hsu and Yang (2002), and Chang et al. (2010).

Sepal Break-Strength Analysis

For sepal break-strength analysis, a single flower sepal was clipped with a small clamp that was attached to a Brookfield CT3-4500 Break-Strength Meter (Brookfield Engineering Laboratories, Inc.). The sepal break strength was the measurement of the force necessary to remove the sepal from the flower, and it was measured using the CT3-4500 Break-Strength Meter. The flower position was counted starting from the first flower with visible white petals at the top of the inflorescence.

Ethylene Responses

For ethylene responses, mature wild-type and transgenic Arabidopsis plants were sealed in plastic chambers and gassed with air or air containing 10 μL L^{-1} ethylene for 3 d in a 16-h-light/8-h-dark cycle as described previously (Chen and Bleecker, 1995; Chen et al., 2011).

RNA Isolation and Real-Time PCR Analysis

Total RNA isolated from Arabidopsis plants used for RT-PCR analysis is described below. All of the equipment was sterilized two times and baked at 180°C for 12 h to prevent Rnase contamination. Plant tissues were ground to a fine power under liquid nitrogen and mixed with 1 mL of TRIzol Reagent (Invitrogen) to homogenize and lyse samples. A volume of 200 μL of chloroform was added into the lysate, incubated at room temperature for 5 min, and then, centrifuged at 13,000g for 10 min at 4°C. The supernatant was transferred to a new 1.5-mL tube, and an equal volume of isopropanol was added to precipitate RNA for 20 min at 4°C. After centrifugation at 13,000g for 10 min at 4°C, the supernatant was discarded, and the RNA pellet was suspended by 75% (v/v) ethanol and centrifuged at 7,500g for 5 min at 4°C. The RNA pellet was vacuum dried for 5 min to remove residual trace of ethanol and dissolved in 20 μL of diethyl pyrocarbonate-treated water.

For real-time quantitative RT-PCR, the reaction was performed on an MJ Opticon System (MJ Research) using SYBER Green Real-Time PCR Master Mix (TOYOBO Co., LTD.). The amplification condition was as described previously (Chen et al., 2011). Sequences for the primers used for real-time quantitative RT-PCR for *FYF* (At5g62165), *FUF1* (At1g71450), *IDA* (At1g68765), *HAESA* (At4g28490), *HSL2* (At5G65710), *HWS* (At3G61590), *BOP1* (At3g57130), *BOP2* (At2g41370), *EDF1* (At1g25560), *EDF2* (At1g68840), *EDF3* (At3g25730), *EDF4* (At1g13260), *SAG12* (At5G45890), *AtMC1* (At1G02170), *AtMC9* (At5G04200), α-*VPE* (At2G25940), and β-*VPE* (At1G62710) are listed in Supplemental Table S7. The housekeeping gene *UBIQUITIN10* (*UBQ10*) was used as normalization control with the following primers: RT-UBQ10-1 and RT-UBQ10-2. All experiments were repeated at least two times as biological replicates for reproducibility. Data were analyzed using Gene Expression Macro software (version 1.1; Bio-Rad).

Construction of the *FYF+GR* Construct and Microarray Analysis

For the *35S:FYF+GR* construct, the cDNA for *FYF* was obtained by PCR amplification and sequence confirmed. The primers contained the *Bam*HI recognition site to facilitate the cloning of the cDNA. The *Bam*HI fragment containing the cDNA was cloned into the PBIGR plasmid upstream of the GR sequence under the control of the CaMV 35S promoter and used for plant transformation. Sequences for the primers are listed in Supplemental Table S7. For microarray analysis, inflorescence from *35S:FYF+GR* Arabidopsis was cut and placed into the water containing 5 μM DEX for 6 h before the isolation of RNA. Total RNA was isolated from all the flower buds before opening of DEX-treated and -untreated *35S:FYF+GR* Arabidopsis by TRIzol Reagent (Invitrogen) according to the manufacturer's protocol; 0.5 g of total RNA derived from paired RNA samples from DEX-treated and -untreated *35S:FYF+GR* Arabidopsis was amplified by a Low RNA Input Fluor Linear Amp Kit (Agilent Technologies) and labeled with Cy3 or Cy5 (CyDye; PerkinElmer) during the in vitro transcription process. CyDye-labeled complementary RNA was fragmented to an average size of about 50 to 100 nucleotides by incubation with fragmentation buffer at 60°C for 30 min. Correspondingly fragmented labeled complementary RNA is then pooled and hybridized to Agilent Arabidopsis 3 Oligo 4x44K Microarray (Agilent Technologies) at 60°C for 17 h. After washing and drying by nitrogen gun blowing, microarrays are scanned with an Agilent Microarray Scanner (Agilent Technologies) at 535 nm for Cy3 and 625 nm for Cy5. Scanned images are analyzed by Feature Extraction 9.5.3 Software (Agilent Technologies), an image analysis and normalization software that is used to quantify signal and background intensity for each feature; it substantially normalized the data by rank-consistency-filtering locally weighted scatterplot smoothing method. The microarray experiments were done three times, and the data analysis described above was done by Welgene Biotech.

Microarray data from this article can be found in the National Center for Biotechnology Information Gene Expression Omnibus under accession number GSM1700867.

Supplemental Data

The following supplemental materials are available.

Supplemental Figure S1. A protein sequence comparison of EDF1/2/3/4, which is in the RAV family of the AP2/ERF-relative proteins.

Supplemental Figure S2. GUS staining patterns in *FYF:GUS* Arabidopsis plants.

Supplemental Figure S3. GUS staining patterns in *EDFs:GUS* Arabidopsis plants and the detection of *EDFs* expression in flowers at different developmental stages.

Supplemental Figure S4. The detection of senescence-associated gene expression in *35S:EDFs+SRDX* plants.

Supplemental Figure S5. A phenotypic analysis of flower senescence and abscission in *etr1-1* mutants ectopically expressing the *EDFs+SRDX* constructs.

Supplemental Figure S6. A phenotypic analysis of flower senescence and abscission in *ein2-1* mutants ectopically expressing the *EDFs+SRDX* constructs.

Supplemental Figure S7. The ectopic expression of *FYF+GR* delayed flower senescence and abscission after DEX treatment.

Supplemental Figure S8. A protein sequence comparison of FUF1 (AtERF21) and four other ERF proteins (AtERF19, AtERF95, AtERF96, and AtERF98) with transcripts that are up-regulated by *FYF*.

Supplemental Figure S9. An analysis of the effect of ethylene on leaves of *35S:FUF1* Arabidopsis.

Supplemental Figure S10. Analysis of *FUF1* transfer DNA insertion line SALK_136922.

Supplemental Table S1. Position of flower that showed senescence/abscission in the *35S:EDFs* Arabidopsis.

Supplemental Table S2. Position of flower that showed senescence/abscission in the *35S:EDFs+SRDX* Arabidopsis.

Supplemental Table S3. Position of flower that showed senescence/abscission in the *35S:EDFs+SRDX/etr1-1* Arabidopsis.

Supplemental Table S4. Position of flower that showed senescence/abscission in the *35S:EDFs+SRDX/ein2-1* Arabidopsis.

Supplemental Table S5. Arabidopsis genes up-regulated in the *35S:FYF+GR* Arabidopsis.

Supplemental Table S6. Arabidopsis genes down-regulated in the *35S:FYF+GR* Arabidopsis.

Supplemental Table S7. Oligo nucleotide sequence of primers used in gene cloning and PCR analysis.

LITERATURE CITED

Alonso JM, Stepanova AN, Leisse TJ, Kim CJ, Chen H, Shinn P, Stevenson DK, Zimmerman J, Barajas P, Cheuk R, et al (2003) Genome-wide insertional mutagenesis of *Arabidopsis thaliana*. Science **301**: 653–657

Basu MM, González-Carranza ZH, Azam-Ali S, Tang S, Shahid AA, Roberts JA (2013) The manipulation of auxin in the abscission zone cells of Arabidopsis flowers reveals that indoleacetic acid signaling is a prerequisite for organ shedding. Plant Physiol **162**: 96–106

Bleecker AB, Estelle MA, Somerville C, Kende H (1988) Insensitivity to ethylene conferred by a dominant mutation in *Arabidopsis thaliana*. Science **241**: 1086–1089

Bleecker AB, Patterson SE (1997) Last exit: senescence, abscission, and meristem arrest in *Arabidopsis*. Plant Cell **9**: 1169–1179

Castillejo C, Pelaz S (2008) The balance between CONSTANS and TEMPRANILLO activities determines *FT* expression to trigger flowering. Curr Biol **18**: 1338–1343

Chang KN, Zhong S, Weirauch MT, Hon G, Pelizzola M, Li H, Huang SS, Schmitz RJ, Urich MA, Kuo D, et al (2013) Temporal transcriptional response to ethylene gas drives growth hormone cross-regulation in *Arabidopsis*. eLife **2**: e00675

Chang YY, Kao NH, Li JY, Hsu WH, Liang YL, Wu JW, Yang CH (2010) Characterization of the possible roles for B class MADS box genes in regulation of perianth formation in orchid. Plant Physiol **152**: 837–853

Chen MK, Hsu WH, Lee PF, Thiruvengadam M, Chen HI, Yang CH (2011) The MADS box gene, *FOREVER YOUNG FLOWER*, acts as a repressor controlling floral organ senescence and abscission in *Arabidopsis*. Plant J **68**: 168–185

Chen QG, Bleecker AB (1995) Analysis of ethylene signal-transduction kinetics associated with seedling-growth response and chitinase induction in wild-type and mutant Arabidopsis. Plant Physiol **108**: 597–607

Chen YF, Etheridge N, Schaller GE (2005) Ethylene signal transduction. Ann Bot (Lond) **95**: 901–915

Cho SK, Larue CT, Chevalier D, Wang H, Jinn TL, Zhang S, Walker JC (2008) Regulation of floral organ abscission in *Arabidopsis thaliana*. Proc Natl Acad Sci USA **105**: 15629–15634

Chou ML, Haung MD, Yang CH (2001) *EMF* genes interact with late-flowering genes in regulating floral initiation genes during shoot development in *Arabidopsis thaliana*. Plant Cell Physiol **42**: 499–507

Clough SJ, Bent AF (1998) Floral dip: a simplified method for *Agrobacterium*-mediated transformation of *Arabidopsis thaliana*. Plant J **16**: 735–743

Coll NS, Vercammen D, Smidler A, Clover C, Van Breusegem F, Dangl JL, Epple P (2010) Arabidopsis type I metacaspases control cell death. Science **330**: 1393–1397

Ecker JR (1995) The ethylene signal transduction pathway in plants. Science **268**: 667–675

González-Carranza ZH, Elliott KA, Roberts JA (2007a) Expression of polygalacturonases and evidence to support their role during cell separation processes in *Arabidopsis thaliana*. J Exp Bot **58**: 3719–3730

González-Carranza ZH, Rompa U, Peters JL, Bhatt AM, Wagstaff C, Stead AD, Roberts JA (2007b) *Hawaiian skirt*: an F-box gene that regulates organ fusion and growth in Arabidopsis. Plant Physiol **144**: 1370–1382

González-Carranza ZH, Shahid AA, Zhang L, Liu Y, Ninsuwan U, Roberts JA (2012) A novel approach to dissect the abscission process in Arabidopsis. Plant Physiol **160**: 1342–1356

Graham LE, Schippers JHM, Dijkwel PP, Wagstaff C (2012) Ethylene and senescence processes. *In* MT McManus, ed, The Plant Hormone Ethylene: Annual Plant Reviews, Vol 44. Wiley-Blackwell, Oxford, pp 305–341

Hepworth SR, Zhang Y, McKim S, Li X, Haughn GW (2005) BLADE-ON-PETIOLE-dependent signaling controls leaf and floral patterning in *Arabidopsis*. Plant Cell **17**: 1434–1448

Hsu HF, Yang CH (2002) An orchid (*Oncidium* Gower Ramsey) *AP3*-like MADS gene regulates floral formation and initiation. Plant Cell Physiol **43**: 1198–1209

Hsu WH (2012) Functional analysis of genes regulating cell division and gametophyte development in Arabidopsis. PhD dissertation. National Chung Hsing University, Taichung, Taiwan, China

Huang Y, Li H, Hutchison CE, Laskey J, Kieber JJ (2003) Biochemical and functional analysis of CTR1, a protein kinase that negatively regulates ethylene signaling in *Arabidopsis*. Plant J **33**: 221–233

Ikeda M, Ohme-Takagi M (2009) A novel group of transcriptional repressors in Arabidopsis. Plant Cell Physiol **50**: 970–975

Ishiguro S, Kawai-Oda A, Ueda J, Nishida I, Okada K (2001) The *DEFECTIVE IN ANTHER DEHISCENCE1* gene encodes a novel phospholipase A1 catalyzing the initial step of jasmonic acid biosynthesis, which synchronizes pollen maturation, anther dehiscence, and flower opening in Arabidopsis. Plant Cell **3**: 2191–2209

Jefferson RA, Kavanagh TA, Bevan MW (1987) GUS fusions: beta-glucuronidase as a sensitive and versatile gene fusion marker in higher plants. EMBO J **6**: 3901–3907

Kieber JJ, Rothenberg M, Roman G, Feldmann KA, Ecker JR (1993) *CTR1*, a negative regulator of the ethylene response pathway in *Arabidopsis*, encodes a member of the raf family of protein kinases. Cell **72**: 427–441

Liljegren SJ (2012) Organ abscission: exit strategies require signals and moving traffic. Curr Opin Plant Biol **15**: 670–676

Lumba S, Tsuchiya Y, Delmas F, Hezky J, Provart NJ, Shi Lu Q, McCourt P, Gazzarrini S (2012) The embryonic leaf identity gene *FUSCA3* regulates vegetative phase transitions by negatively modulating ethylene-regulated gene expression in Arabidopsis. BMC Biol **10**: 8

McKim SM, Stenvik GE, Butenko MA, Kristiansen W, Cho SK, Hepworth SR, Aalen RB, Haughn GW (2008) The *BLADE-ON-PETIOLE* genes are essential for abscission zone formation in *Arabidopsis*. Development **135**: 1537–1546

Murashige T, Skoog F (1962) A revised medium for rapid growth and bioassays with tobacco tissue cultures. Physiol Plant **15**: 473–497

Nakano T, Suzuki K, Fujimura T, Shinshi H (2006) Genome-wide analysis of the ERF gene family in Arabidopsis and rice. Plant Physiol **140**: 411–432

Noh YS, Amasino RM (1999) Identification of a promoter region responsible for the senescence-specific expression of SAG12. Plant Mol Biol **41**: 181–194

Norberg M, Holmlund M, Nilsson O (2005) The *BLADE ON PETIOLE* genes act redundantly to control the growth and development of lateral organs. Development **132**: 2203–2213

Patterson SE, Bleecker AB (2004) Ethylene-dependent and -independent processes associated with floral organ abscission in Arabidopsis. Plant Physiol **134**: 194–203

Peng YJ, Shih CF, Yang JY, Tan CM, Hsu WH, Huang YP, Liao PC, Yang CH (2013) A RING-type E3 ligase controls anther dehiscence by activating the jasmonate biosynthetic pathway gene *DEFECTIVE IN ANTHER DEHISCENCE1* in *Arabidopsis*. Plant J **74**: 310–327

Roberts JA, Elliott KA, Gonzalez-Carranza ZH (2002) Abscission, dehiscence, and other cell separation processes. Annu Rev Plant Biol **53**: 131–158

Rogers HJ (2013) From models to ornamentals: how is flower senescence regulated? Plant Mol Biol **82**: 563–574

Rojo E, Martín R, Carter C, Zouhar J, Pan S, Plotnikova J, Jin H, Paneque M, Sánchez-Serrano JJ, Baker B, et al (2004) VPEgamma exhibits a caspase-like activity that contributes to defense against pathogens. Curr Biol **14**: 1897–1906

Sakuma Y, Liu Q, Dubouzet JG, Abe H, Shinozaki K, Yamaguchi-Shinozaki K (2002) DNA-binding specificity of the ERF/AP2 domain of Arabidopsis DREBs, transcription factors involved in dehydration- and cold-inducible gene expression. Biochem Biophys Res Commun **290**: 998–1009

Schaller GE (2012) Ethylene and the regulation of plant development. BMC Biol **10**: 9

Shi CL, Stenvik GE, Vie AK, Bones AM, Pautot V, Proveniers M, Aalen RB, Butenko MA (2011) *Arabidopsis* class I KNOTTED-like homeobox proteins act downstream in the IDA-HAE/HSL2 floral abscission signaling pathway. Plant Cell **23**: 2553–2567

Stenvik GE, Tandstad NM, Guo Y, Shi CL, Kristiansen W, Holmgren A, Clark SE, Aalen RB, Butenko MA (2008) The EPIP peptide of INFLORESCENCE DEFICIENT IN ABSCISSION is sufficient to induce abscission in *Arabidopsis* through the receptor-like kinases HAESA and HAESA-LIKE2. Plant Cell **20**: 1805–1817

Stepanova AN, Alonso JM (2005) *Arabidopsis* ethylene signaling pathway. Sci STKE **2005**: cm4

Tzeng TY, Yang CH (2001) A MADS box gene from lily (*Lilium Longiflorum*) is sufficient to generate dominant negative mutation by interacting with PISTILLATA (PI) in *Arabidopsis thaliana*. Plant Cell Physiol **42**: 1156–1168

Wagstaff C, Yang TJ, Stead AD, Buchanan-Wollaston V, Roberts JA (2009) A molecular and structural characterization of senescing Arabidopsis siliques and comparison of transcriptional profiles with senescing petals and leaves. Plant J **57**: 690–705

Wang F, Cui X, Sun Y, Dong CH (2013) Ethylene signaling and regulation in plant growth and stress responses. Plant Cell Rep **32**: 1099–1109

Woo HR, Kim JH, Kim J, Kim J, Lee U, Song IJ, Kim JH, Lee HY, Nam HG, Lim PO (2010) The RAV1 transcription factor positively regulates leaf senescence in Arabidopsis. J Exp Bot **61**: 3947–3957

Wu XM, Yu Y, Han LB, Li CL, Wang HY, Zhong NQ, Yao Y, Xia GX (2012) The tobacco *BLADE-ON-PETIOLE2* gene mediates differentiation of the corolla abscission zone by controlling longitudinal cell expansion. Plant Physiol **159**: 835–850

Xu ZS, Chen M, Li LC, Ma YZ (2011) Functions and application of the AP2/ERF transcription factor family in crop improvement. J Integr Plant Biol **53**: 570–585